J. Condensed Matter Nucl. Sci. 29 (2019) 219–229

Research Article

Uranium Fission Using Pd/D Co-deposition

Pamela A. Mosier-Boss* and Lawrence P. Forsley
Global Energy Corporation, San Diego, CA 92123, USA

Patrick McDaniel
University of New Mexico, Albuquerque, NM 87131, USA

Abstract

In this investigation, we explored using Pd/D generated energetic particles to fission uranium. Analysis of the CR-39 microphotographs liquid scintillation counter (LSC) alpha and beta spectra, and high purity germanium (HPGe) spectral gamma data support fissioning of U-238/U-235 implying that a hybrid fusion-fission reactor based upon Pd/D co-deposition could be feasible.
 ISSN 2227-3123

Keywords: CR-39, HPGe, Hybrid reactor, LSC, Uranium

1. Introduction

Earlier, we reported on observing the production of energetic particles during Pd/D co-deposition [1,2]. The energetic particles produced include ≥1.8 MeV protons (including 15 MeV protons), ≥7 MeV alphas, 2.2–2.5 MeV neutrons, and secondary particles from either energetic protons and/or neutrons. We have also reported on observing the production of ≥9.6 MeV neutrons [3]. The Java-based Nuclear Information Software (JANIS) database [4] indicates that these particles are energetic enough to fission both U-238 and U-235. In this investigation, we explored using Pd/D generated energetic particles to fission uranium. An experiment was conducted in which Pd/D co-deposition was done on a Au/U composite cathode. Both real-time high purity germanium (HPGe) and a CR-39 detector were used to monitor the reaction. A month after the reaction was completed, HPGe spectra of the U wire and the Au wire and deposit at the end of the experiment were obtained in a Compton suppressed cave. Three months after termination of the experiment, liquid scintillation measurements of the deposit as a function of time were made. The results of those measurements are discussed in this communication.

*Corresponding author. E-mail: pboss@san.rr.com.

 ISSN 2227-3123

2. Experimental

Pd/D co-deposition was done on a Au/U (natural uranium 0.71% U-235) composite cathode that was in contact with a CR-39 detector. The cell was placed inside a Pb cave close to a HPGe detector. Upon termination of the experiment, the CR-39 detector was etched as previously described [1,3] and underwent microscopic examination. A month after the experiment was terminated, HPGe spectra of the native wire as well as the Au cathode and deposit were obtained at the University of Texas, Austin. Spectra were obtained using a 30% HPGe detector in a Compton suppressed cave [5–7]. Compton suppression systems are typically used to reduce the background continuum as well as the cosmic and natural background. Three months after termination of the experiment, samples of the deposit were placed in 10 mL of scintillating (Scintiverse^{TM}) cocktail and liquid scintillation spectra were obtained periodically over a period of 550 days.

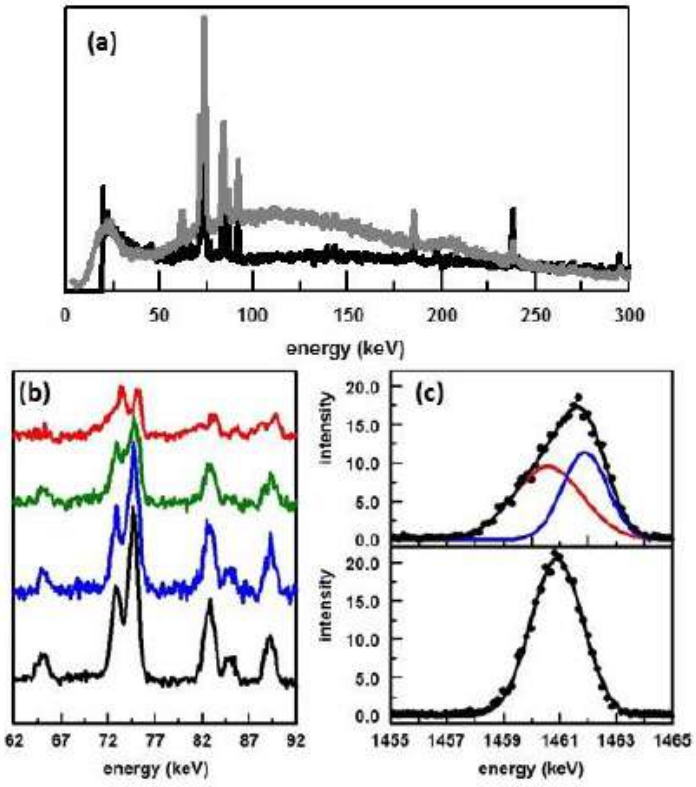

Figure 1. Gamma ray spectra obtained during the experiment where: (a) spectra of the Pb cave (*black spectrum*) and the electrochemical cell obtained on Feb. 28 at 08:30 (*gray spectrum*); (b) time normalized, baseline corrected spectra obtained at (*bottom to top*) Feb. 28 at 08:30, Feb. 28 at 13:00, Feb. 28 at 17:38, and Feb. 29 at 11:14; and (c) time normalized, baseline corrected spectra of the K-40 line obtained on Feb. 28 at 08:30 (*bottom*) and Feb. 29 at 11:14 (*top*).

3. Results and Discussion

3.1. Real-time HPGe spectra

Figure 1a shows gamma ray spectra of the Pb cave and the cell after 33.5 h of electrolysis. At this point the cell current is at –0.4 mA. The HPGe detector has an Al window that cuts off at 20 keV. This cut-off is evident in the background spectrum of the Pb cave. The spectrum of the cell shows background lines observed on top of a raised baseline. Three broad peaks at ∼20, 118, and 194 keV are observed on this raised baseline. With additional time, these broad peaks disappeared. The spectrum of the cell clearly shows counts below the cut-off of the Al window. These counts and the broadness of the three bands making up the baseline cannot be due to gamma rays and are caused by something interacting with the detector itself. Neutrons are the only thing that can pass through the Al window and interact with the Ge atoms of the detector.

Further evidence of neutron damage to the detector is shown in Fig. 1b,c. These spectra have been time normalized and the background has been corrected. The times the spectra were collected are indicated in the figure caption. Figure 1b shows peaks due to the Pb lines and background peaks. On Feb. 28 at 08:30 and at 13:00, the peaks are intense and cleanly resolved. By Feb. 28 at 17:28, the peaks are less intense and are broadening. On Feb. 29 at 11:14, the peaks are clearly less intense and have broadened. Figure 1c shows the K-40 line. On Feb. 28 at 08:30, the K-40 line is symmetrical and fits to a single Gaussian line. The K-40 peak observed on Feb. 29 at 11:14 has lost intensity and shows a tail on the low frequency side of the peak. Its line shape is described by the sum of two Gaussian lines, shown in Fig. 1c. The changes observed in the gamma lines are consistent with neutron damage to the HPGe detector [8].

Inelastic scattering of neutrons on Ge-74 and Ge-72 cause broad asymmetric gamma peaks at 596 and 691.3 keV, respectively, when the energy of the neutrons are $\leq$1 MeV [9]. For neutrons with energies $\geq$1 MeV, these lines broaden and flatten out. When neutron energies are greater than 4 MeV these peaks cannot be separated from the background. No peaks at 596 and 691.3 keV were observed for the electrolyzing cell. Therefore, the average energy of the neutrons generated during electrolysis is greater than 4 MeV. Another way to estimate the average neutron energy is to model the neutron elastic scattering of the Ge nuclei using the Monte–Carlo technique [10,11]. When a high energy neutron elastically scatters a germanium nucleus, it leaves an ionization trail that is proportional to the energy given to each germanium nuclei encountered. Germanium recoil spectra, based on isotropic elastic scattering, were calculated for fission neutrons (2 MeV) and 6.3–6.83 MeV neutrons. The results of these calculations are summarized in Fig. 2. The baseline measured on Feb. 28 at 08:30 more closely resembles the recoil spectrum for the 6.3–6.83 MeV neutrons than the fission neutrons. Radiation hardness refers to higher energy particles, be they gammas, protons, neutrons, etc. The degree of hardness is determined by taking the ratio of the total counts in the 100–300 keV energy range with those in the 50–100 keV energy range [12]. The higher the ratio, the harder the spectrum. As can be seen from Fig. 2, the Pd/U/D neutron energy spectrum is harder than that from fission alone. This hardness of the spectrum indicates a larger contribution of higher energy neutrons to the Pd/U/D neutron energy spectrum and that there is another source of neutrons than fissioning of uranium.

3.2. CR-39 results

The CR-39 detector in contact with the Au/U/Pd composite cathode was etched and underwent microscopic examination. Figure 3 shows some examples of elongated tracks as well as triple tracks that were observed in the detector used in the U experiment. Also shown are their corresponding DT neutron-generated tracks. More elongated and triple tracks were observed in the detector used in the U experiment than in previous Pd/D co-deposition experiments [1,3,13]. This indicates that more neutrons were generated in the Au/U/Pd/D experiment than in any Pd/D experiments. The elongated track shown in Fig. 3 is due to proton recoils. From the length of the track, it is possible to

estimate that the energy of the neutron that generated it was greater than 0.114 [14]. Triple tracks are diagnostic of the carbon break-up reaction, $^{12}C(n,n')3\alpha$, which has an energy threshold for the neutron of $\geq$9.6 MeV [15]. These neutron energies are in agreement with the estimate made from the real-time HPGe measurements.

Large (40 μm long and 10 μm wide) shallow cylindrical tracks similar to the one shown in Fig. 4a were observed in the CR-39 detector used in the Au/U/Pd/D experiment. Such tracks have neither been observed in CR-39 detectors in contact with a bare U wire nor in CR-39 detectors used in Pd/D co-deposition experiments. Since these tracks have not been observed in Pd/D co-deposition experiments, uranium is the source of these tracks in the Au/U/Pd/D experiment. The large size and shallowness of the track indicates that it was caused by a high Z particle [16]. Such high Z particles would be created when uranium fissions. To verify this, a piece of native uranium wire was placed in contact with a CR-39 detector and irradiated for 4.5 h with DT neutrons. After etching, large cylindrical tracks, due to high Z fission fragments, were observed (Fig. 4b). The presence of these tracks in the detector used in the Au/U/Pd/D experiment indicates that fissioning of U has occurred and that they aren't the result of either DT neutrons alone or actinide alpha decay.

3.3. Post HPGe analysis in a Compton suppressed cave

A month after the experiment was terminated, HPGe spectra were obtained of the native U wire as well as the cathode and deposit remaining at the end of the experiment. These spectra were obtained in a Compton suppressed system at the University of Texas, Austin. Spectra are shown in Fig. 5. Identification of major lines are indicated. Clearly changes are observed in the spectrum after the U has undergone electrolysis that will be discussed *vide infra*. Gamma lines due to U-235, Th-231, and Th-234 are identified [17]. Th-231 and Th-234 arise from the decay of U-235 and U-238, respectively [18].

Figure 6 shows an expansion of the region between 60 and 120 keV. The Th and U X-ray lines are identified. It can be seen that the ratios of the Th gamma lines and the Th X-ray lines are the same for both spectra of the bare U wire and the spent cathode. Compared to the Th lines, there is clearly a decrease in the U X-ray lines in the spectrum of the spent cathode, Fig. 6. In Fig. 5, the ratio of the U-235 gamma lines and Th gamma and X-ray lines are the same for both spectra. From this it can be concluded that the decrease in the U X-ray lines cannot be due to uranium accumulating on the anode otherwise a similar decrease in the U-235 gamma lines would have been observed. Also,

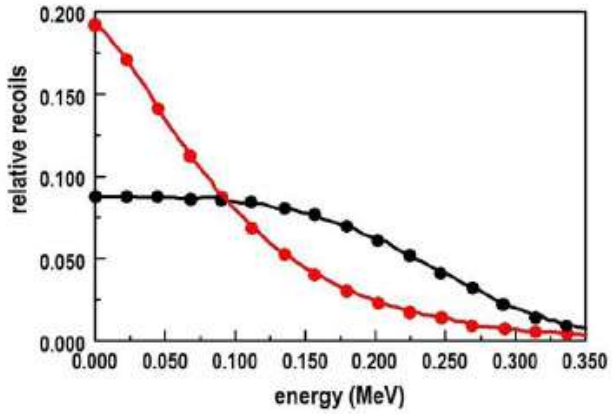

Figure 2. Germanium recoil spectra, based on isotropic elastic scattering, calculated for fission neutrons (*red spectrum*) and 6.3–6.83 MeV neutrons (*black spectrum*) using the Monte–Carlo technique.

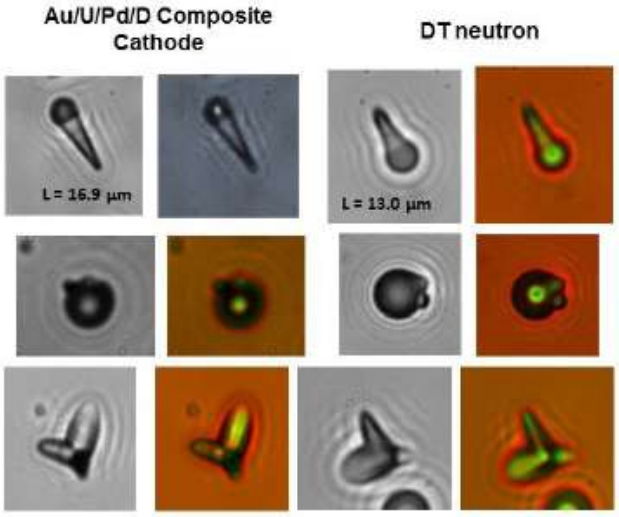

Figure 3. Photomicrographs of tracks observed in CR-39 detectors used in Pd/D co-deposition experiment conducted on an Au/U cathode and their corresponding DT neutron generated tracks. Magnification 1000× . The left-hand images were obtained by focusing the optics on the surface of the detector while the right-hand images are overlays of two images taken at two different focal lengths (*surface and bottom of the pits*). Lengths (L) of the recoil proton tracks are indicated.

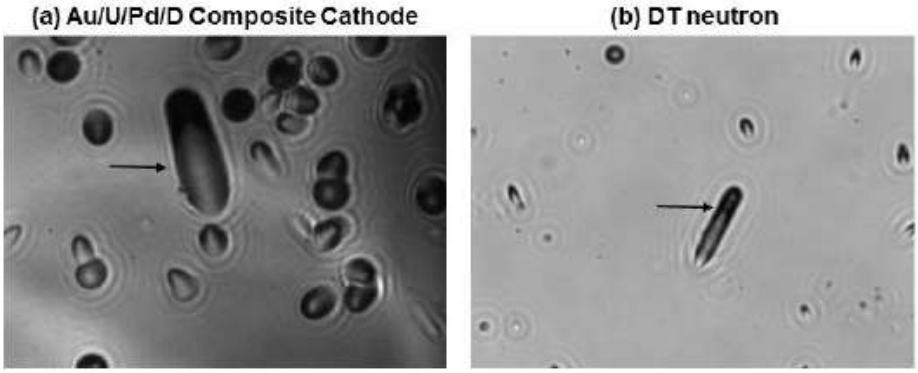

Figure 4. Photo micrographs of CR-39 detector that had been used in a Pd/D co-deposition experiment conducted on an Au/U cathode (a) and a detector that had been in contact with uranium wire exposed to DT neutrons (b). Magnification for both is 1000×. Arrows indicate tracks due to high Z fragments. The detector used in the co-deposition experiment had been etched for 6 h while the detector exposed to DT neutrons had been etched for 1 h.

no deposit was observed on the anode upon termination of the experiment. Since no changes were observed for the Th X-ray lines, the decrease in the U X-ray lines cannot be due to occlusion. Therefore, a decrease in the uranium X-ray peaks suggests that uranium has been consumed. As was discussed vide supra, the CR-39 detector next to the cathode showed large tracks attributed to large Z fission fragments (Fig. 4). These fragments came from fissioning of the uranium. Therefore, the decrease in the uranium X-ray lines provides further support that uranium has been

fissioned. Furthermore, U-238 has been preferentially fissioned. Although both U-235 and U-238 will contribute to the U X-ray lines, the primary contributor is U-238 since its concentration in native U is two orders of magnitude greater than U-235. Since no change was observed in the ratio of the U-235 gamma lines compared to the Th lines, Fig. 5, it can be concluded that U-238 was fissioned.

Between 65 and 81 keV, five new lines are observed in the spectrum obtained for the spent cathode, (Fig. 6). Based on the relative intensities and positions of these lines, they are attributed to the Kα and Kβ X-ray lines of Au [17]. These are stimulated X-rays that are generated by the refilling of the K shell electron orbits ionized by the passage of charged particles or higher energy gamma rays [19].

Figure 7 shows expansions of the regions between 30–130 and 90–130 keV regions of Fig. 5. In the 90–130 keV region, three new peaks at 102.18, 105.79, and 121.37 keV are observed in the spectrum of the cathode/deposit. The peak at 121.37 keV is broader than the other two peaks and is probably comprised of overlapping peaks. Based upon the positions and relative intensities of these peaks, they have been assigned to the Kα and Kβ X-ray lines of Am [16]. Like the Au X-ray lines, these are stimulated X-ray lines for Am. As in the case of Au, these Am X-ray lines are stimulated by the alpha and gamma emissions of U-235/U-238 and their daughters. In the region between 30 and 130 keV, a small peak at ~59 keV is observed. This peak is attributed to the gamma emission of Am-241, which happens to be the most intense line of Am-241 [16]. The fact that the line due to the gamma emission of Am-241 is smaller than the stimulated Am X-ray lines is probably due to absorption of this gamma emission and induced fluorescence of lower energy X-ray lines [19]. Furthermore, there should be no correlation between the magnitude of a gamma line from the nucleus and the X-ray lines from electron transitions in the shells surrounding the nucleus. The most likely reaction pathways for the production of Am-241 are [20,21]:

$$^{238}_{92}\mathrm{U} + \mathrm{n} \rightarrow ^{239}_{92}\mathrm{U} \xrightarrow[23.5\,\mathrm{min}]{\beta^-} ^{239}_{93}\mathrm{Np} \xrightarrow[2.356\,\mathrm{days}]{\beta^-} ^{239}_{94}\mathrm{Pu} \xrightarrow{\mathrm{n},\gamma} ^{240}_{94}\mathrm{Pu} \xrightarrow{\mathrm{n},\gamma} ^{241}_{94}\mathrm{Pu} \xrightarrow[14.35\,\mathrm{years}]{\beta^-} ^{241}_{95}\mathrm{Am}.$$

The production of Am indicates that the neutron kinetic energy has to be < 1 MeV, which is the cross-section threshold favoring capture over fission in U-238, in order to create Pu-239 [4]. Production of Am indicates that there was a high flux of neutrons, which is in agreement with the CR-39 data.

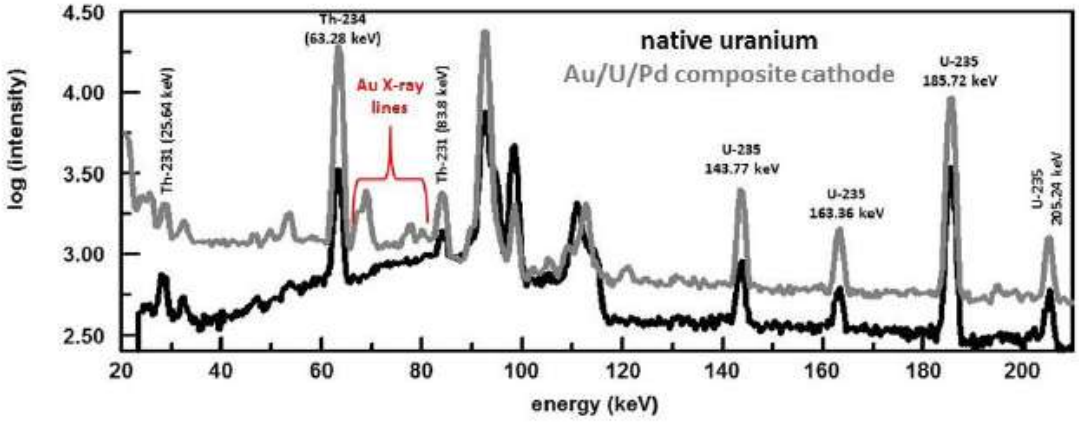

Figure 5. Gamma ray spectra of the native uranium wire (*black*) and the Au/U/Pd composite cathode (*gray*) at the end of the experiment. Peak assignments are shown [17].

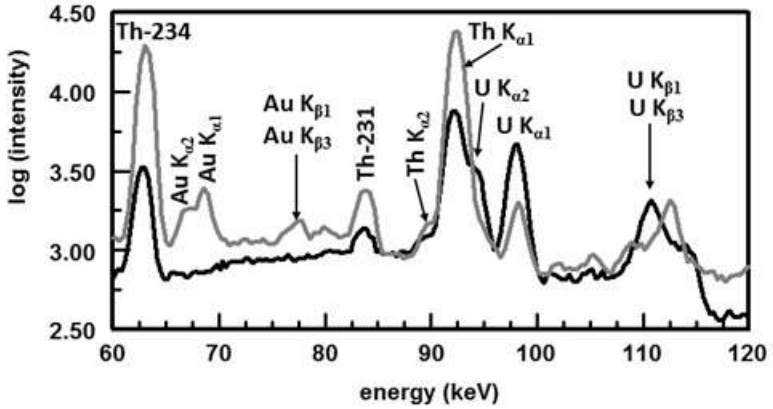

Figure 6. Gamma ray spectra, between 60 and 120 keV, of the native uranium wire (*black*) and the Au/U/Pd composite cathode (*gray*) at the end of the experiment. Peak assignments are shown [17].

3.4. Post liquid scintillation counting (LSC) analysis of the deposit

Fissioning of uranium produces several hundred radionuclides [22,23]. Most isotopes in the fission products have extra neutrons and tend to decay to more stable isotopes through β emission accompanied by γ emission. Three months after the experiment was terminated, the use of LSC was explored to measure these beta emissions. However, alpha and gammas will also stimulate photon emissions from these cocktails. The three types of radiation interact differently

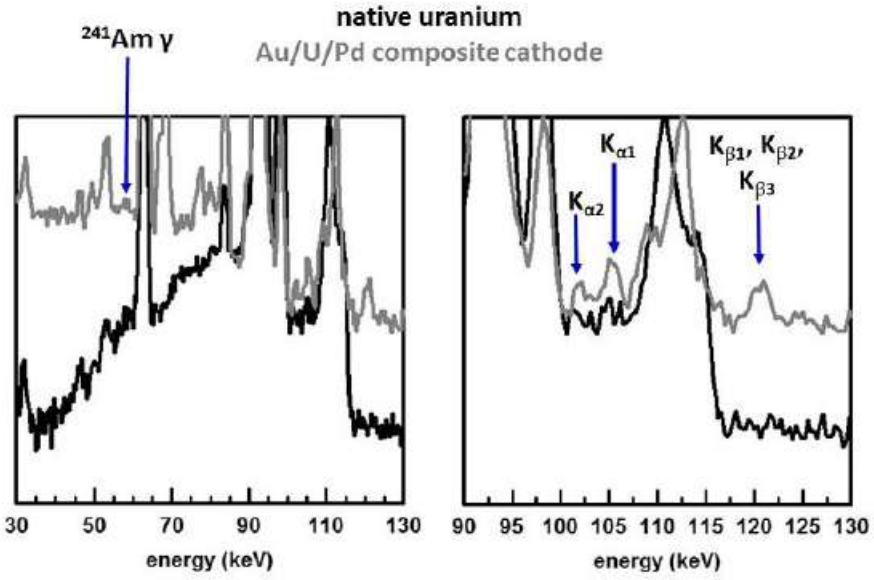

Figure 7. Expansions of the 30–130 and 90–130 keV regions of the HPGe spectra shown in Fig. 5. Peak assignments are shown.

with the liquid scintillator. For a mixture of alpha, beta, and gamma emitters, the resultant spectrum is comprised of a relatively narrow alpha peak sitting atop a beta–gamma continuum [24]. A Beckman Coulter LS6500 multipurpose scintillator counter was used to make these measurements. This counter has two diametrically opposed photomultplier tubes (PMTs). In order to be detected, the photons created by the interaction of the fluor with the radioactive nuclide need to be within the line of sight of the PMTs allowing coincidence counting.

Upon termination of the experiment, there was no evidence of the U wire in the cathode. Formation of uranium hydride/deuteride results in the complete disintegration of the structure of the original metal and the hydride/deuteride appears as a voluminous, finely divided black powder [25]. This break-up of the uranium wire during electrolysis will cause disequilibrium between U-235/U-238 and their daughters. This will cause changes in the LSC spectra as these species in the decay chains come back to equilibrium. So, besides what happened to the uranium wire during electrolysis and Pd/D co-deposition, disequilibrium will be occurring as well. To determine the effect of disequilibrium, a piece of native U wire was placed in an aqueous solution of LiCl. This caused the wire to break-up into particles which will cause disequilibrium. Some of these particles were placed in the cocktail and spectra were measured periodically over a period of 195 days. These spectra are shown in Fig. 8a. Initially, the LSC spectra of the particles show a beta–gamma continuum. Then a fairly narrow peak grows in at channel 675. This narrow peak is due to the alpha emission of U-234. It takes a while for this peak to grow in as uranium has to dissolve into solution in order for the alphas to be seen. This is because the path length for 5 MeV alpha particles in a liquid scintillator solution is approximately 50 μm [26]. Consequently, unless the particles were directly between the windows of the PMTs, no photons would be detected. As shown in Fig. 8a, no peak due to the alpha of U-238 is seen, which is due to the fact that the sample is in disequilibrium [27]. Since the half-life of U-234 ($t_{1/2} = 2.5\times 10^5$ years) is shorter than that of U-238 ($t_{1/2} = 4.5\times 10^8$ years), the U-238 peak is less intense than the U-234 peak when in disequilibrium and is obscured by the other emissions of the beta–gamma continuum [26]. With time another alpha peak grows in at channel 625. This peak is due to U-238. It keeps growing until the sample reaches equilibrium. As shown in Fig. 8a, no significant changes are observed for the rest of the LSC spectra.

Figure 8b shows LSC spectra obtained of the deposit as a function of time. It is completely different that the spectra

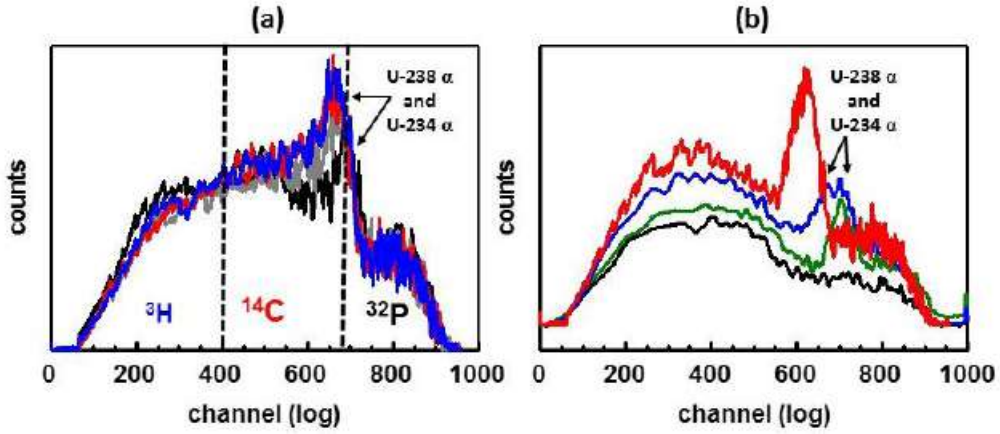

Figure 8. Liquid scintillator spectra taken as a function of time for (a) uranium particles formed by immersing a piece of native uranium wire in an aqueous LiCl solution (spectra taken after 1, 125, 182, and 195 days) and (b) the deposit as a result of the Pd/D co-deposition experiment conducted on a Au/U cathode (spectra taken after 0, 9, 85, and 356 days). Channels for ^{3}H, ^{14}C, and ^{32}P are indicated as are the alpha peaks for U-234 and U-238. Energies of these alphas are 4.2 and 4.7 Mev for U-238 and U-234, respectively.

obtained by the U particles shown in Fig. 8a. Initially no alpha peaks are observed. With time the alpha peaks due to U-234 and U-238 grow in as the uranium goes into solution. With additional time, another alpha peak at a lower energy than that for U-238 begins to grow in (Fig. 8b). After 355 days in the cocktail, this peak reaches maximum height. The energy of this peak is estimated to be 3.2 $\pm$ 0.3 MeV. The species responsible for this alpha peak must be long-lived. The only long-lived species that have an alpha emission near 3.2 MeV are Pt-190 ($t_{1/2} = 6.5 \times 10^{11}$ years) and Gd-148 ($t_{1/2} = 74.6$ years) [17]. Based on the intensity of the alpha peak, it is most likely due to Gd-148 as it has a much shorter half-life and it is a fission product, whereas Pt-190 is not. Besides these alphas, increases in the beta–gamma continuum are observed with time as more species leach from the deposit. These species are clearly different than what was observed for the U particles and are attributed to long-lived fission products.

4. Conclusions

The use of energetic particles produced during Pd/D co-deposition to fission uranium was explored. Real-time HPGe spectral data obtained during the early stages of the plating phase of Pd/D co-deposition on a Au/U composite cathode showed evidence of neutron damage. Using the Monte–Carlo technique, the average energy of the neutrons was estimated to be of the order of 6–7 MeV. A gamma ray spectrum obtained in a Compton suppressed Pb cave a month after the experiment showed the presence of Am-241 which is likely created by neutron capture by U-238 to form Pu-239. Pu-239 undergoes successive neutron captures to form Pu-241 which then beta decays into Am-241. The HPGe spectra also shows a decrease in the U X-ray peaks indicating that U has been consumed. Production of energetic neutrons and fissioning of U-238/U-235 were further verified by the CR-39 detector that was in contact with the Au/U/Pd composite cathode. LSC spectra showed evidence of an alpha emitter at 3.2 $\pm$ 0.3 that is likely due to Gd-148. Additional changes in the LSC spectra with time show beta–gamma emitters due to long-lived fission products. These results indicate that uranium can be fissioned by the energetic particles formed as a result of Pd/D co-deposition.

The implication of this experiment is that a hybrid fusion-fission reactor is feasible. The main advantages of such a reactor would be, (1) it does not require enrichment of U-235, (2) it does not produce greenhouse gases, and (3) it can easily be shut off by simply turning off the current to the cell. Such a reactor might also be used to dispose of nuclear wastes and long life radioactive fission products remaining in spent nuclear fuel.

Acknowledgements

This effort was funded by the Defense Threat Reduction Agency (DTRA), and JWK Corporation. The authors would like to thank Mr. Mark Morey, Dr. Jim Tinsley, and Mr. Paul Hurley of National Security Technologies, LLC, Special Technologies Laboratory in Santa Barbara, CA for exposing CR-39 detectors, and uranium in contact with CR-39 detectors, to DT neutrons. The HPGe spectra of the composite cathode and native uranium wire obtained in a Compton suppressed Pb cave were taken by Dr, Sheldon Landsberger of the University of Texas at Austin, Nuclear Engineering Teaching Laboratory. The authors would also like to thank Dr. Gary Phillips, nuclear physicist, retired from the Naval Research Laboratory, US Navy, Radiation Effects Branch for valuable discussions in interpreting the CR-39 data.

References

[1] P.A. Mosier-Boss, F.E. Gordon, L.P. Forsley and D. Zhou, Detection of high energy particles using CR-39 detectors, Part 1: results of microscopic examination, scanning, and LET analysis, *Int. J. Hydrogen Energy* **42** (2017) 416–428.

[2] A.S. Roussetski, A.G. Lipson, E.I. Saunin, F. Tanzella and M. McKubre, Detection of high energy particles using CR-39 detectors, Part 2: results of in-depth destructive etching analysis, *Int. J. Hydrogen Energ* **42** (2017) 429–436.

[3] P.A. Mosier-Boss, S. Szpak, F.E. Gordon and L.P.G. Forsley, Triple tracks in CR-39 as the result of Pd/D co-deposition: evidence of energetic neutrons, *Naturwissenschaften* **96** (2009) 135–142.
[4] JANIS software, http://www.oecd-nea.org/janis/.
[5] M. Petra, G. Swift and S. Landsberger, Design of a Ge NaI(Tl) Compton suppression spectrometer and its use in neutron activation analysis, *Nucl. Instrum. Methods* A **299** (1990) 85–87.
[6] S. Landsberger and S. Peshev, Compton suppression neutron activation analysis: past, present and future, *J. Radioanal. Nucl. Chem.* **202** (1996) 201–224.
[7] G. Nicholson, S. Landsberger, L. Welch and R. Gritzo, Characterization of a Compton suppression system and the applicability of Poisson statistics, *J. Radioanal. Nucl. Chem.* **276** (2008) 577–581.
[8] E.H. Seabury, C. Dew van Siclen, J.B. McCabe, C.J. Wharton and A.J. Caffrey, Neutron damage in mechanically cooled high-purity germanium detectors for field-portable prompt gamma neutron activation analysis (PGNAA) systems, *2013 IEEE Nuclear Science Symposium and Medical Imaging Conference*, Oct. 2013.
[9] G. Fehrehbacher, R. Meckbach, H.G. Paretzke Fast neutron detection with germanium detectors: computation of response functions for the 692 keV inelastic scattering peak, *Nucl. Instrum. Methods* A **372** (1996) 239–245.
[10] J. Ljungvall and J. Nyberg, A study of fast neutron interactions in high-purity germanium detectors, *Nucl. Instum. Methods* A **546** (2005) 553–573.
[11] M. Baginova, P. Vojtyla and P.P. Povinec Investigation of neutron interactions with Ge detectors, *Nucl. Instum. Methods* A **897** (2018) 22–31.
[12] M. Tavani, Euclidean versus non-Euclidean gamma-ray bursts, *Astrophys. J.* **497** (1998) L21–L24.

[13] P.A.Mosier-Boss, J.Y. Dea, L.P.G. Forsley, M.S. Morey, J.R.Tinsley, J.P. Hurley and F.E. Gordon, Comparison of Pd/D co-deposition and DT neutron generated triple tracks observed in CR-39 detectors, *Euro. Phys. J. Appl. Phys*. 51 (2010) 1–11.
[14] G.W. Phillips, J.E. Spann, J.S. Bogard, T. VoDinh, D. Emfietzoglou, R.T. Devine and M. Moscovitch, Neutron spectrometry using CR-39 track etch detectors, *Radiation Prot. Dosim.* **120** (2006) 457–460.
[15] A.M. Abdel-Moneim and A. Abdel-Naby, A study of fast neutron beam geometry and energy distribution using triple-α reactions, *Radiation Meas.* **37** (2003) 15–19.
[16] J.K. Pálfalvi, Y. Akatov, J. Szabó, L. Sajó-Bohus and I. Eördögh, Evaluation of solid state nuclear track detector stacks exposed on the international space station, *Radiation Prot. Dosimetry* **210** (2004) 393–397.
[17] Periodic Table Linked to ToRI data of known isotopes of each element, http://nucleardata.nuclear.lu.se/toi/perchart.htm.
[18] L.P. Forsley, P.A. Mosier-Boss, P.J. McDaniel and F.E. Gordon Charged particle detection in the Pd/D system: CR-39 SSNTD vs. real-time measurement of charged particle stimulated Pd K shell X-rays *Electrochim. Acta* **88** (2013) 373–383.
[19] Decay Chains, http://metadata.berkeley.edu/nuclear-forensics/Decay%20Chains.html
[20] J.W. Kennedy, G.T. Seaborg, E. Segrè and A.C. Wahl, Properties of element 94, *Phys. Rev.* **70** (1946) 555–556.
[21] K. Kostecka, Americium – from discovery to the smoke detector and beyond, *Bull. Hist. Chem.* **33** (2008) 89–93.
[22] G.R. Crocker, Fission product decay chains: schematics with branching fractions, half-lives, and literature references U.S. Naval Radiological Defense Laboratory USNRDL-TR-67-111, 24 Jun. 1967.
[23] B. Li, Analysis of fission products – a method for verification of a CTBT during on-site inspections, *Sci. Global Secur.* **7** (1998) 195–207.
[24] Y. Dazhu, Z. Yongjun, S. Möbius and C. Keller, Simultaneous determination of alpha and beta-emiting nuclides by liquid scintillation counting, J *Radioanal. Nucl. Chem. Lett.* **144** (1990) 63–71.
[25] T. Hashino and Y. Okajima, Mechanism of the reaction of hydrogen with uranium, *J. Phys. Chem.* **77** (1973) 2236–2241.
[26] W.J. McDowell and B.L. McDowell, *Liquid Scintillation Alpha Spectrometry*, CRC Press, Boca Raton, 1994.
[27] H.M. Pritchard and A. Cox, Liquid scintillation screening method for isotopic uranium in drinking water, in H. Ross, J.E. Noakes and J.D. Spaulding (Eds.), *Liquid Scintillation Counting And Organic Scintillators,* Lewis, Michigan, USA, 1991.